Biol. Cybern. 69, 119–128 (1993)

Biological Cybernetics


# Modelling velocity profiles of rapid movements: a comparative study

**Réjean Plamondon, Adel M. Alimi, Pierre Yergeau, Franck Leclerc**

Laboratoire Scribens, Département de Génie Electrique, Ecole Polytechnique de Montréal, C.P. 6079, Succ. 'A', Montréal, Canada, H3C 3A7

Received: 4 September 1992/Accepted in revised form: 4 January 1993

**Abstract.** In this paper we compare 23 different models that can be used to describe the asymmetric bell-shaped velocity profiles of rapid-aimed movements. The comparison is performed with the help of an analysis-by-synthesis experiment over a database of 1052 straight lines produced by nine human subjects. For each line and for each model, a set of parameters is extracted that minimizes the error between the original and the reconstructed data. Performance analysis on the basis of the mean-square-error clearly reflects the superiority of the support-bounded lognormal model to globally describe the velocity profile characterizing rapid movements.

## 1 Introduction

One basic approach in the study of rapid human movements has been the modelling of the movement generation system with the help of different mathematical representations. These models, sometimes called phenomenological, can be very useful from two points of view. From a theoretical perspective, this approach provides a holistic description of the processes, based on an external representation of the phenomena, with the help of a proper set of differential equations or transfer functions. A specific model provides a set of parameters that describes the observed movements under different experimental conditions and so it opens a window on the different processes that occur during these movements, allowing a global interpretation of the phenomena in terms of input commands, control variables, and output functions. From a practical perspective, these models can also be used to segment more complex movements, to compress and store data efficiently and to provide a parametric description of signals that can be used for computer processing applications in pattern recognition and robotics.

*Correspondence to*: R. Plamondon

However, to take advantage of this approach, several questions must be answered. Probably the most important one is. Which is the best model for describing a specific set of rapid-aimed movements? Indeed, all the theoretical and practical advantages of analytical modelling rely on having the most meaningful and powerful set of parameters to represent a specific class of movements.

Many models have been proposed in the past for describing different classes of movements, and it should be expected that, although the goal of each of these studies may have differed, some convergence towards a single, unique and powerful model of rapid movement generation might emerge. As for the modelling of any physical system, it should be expected that a model will ultimately stand or fall on the basis of its agreement or disagreement with experimental findings. To perform such a test, a widely accepted observation must be used as the experimental benchmark, and all the models then tested under the same experimental protocol and with the same database.

In this context, we ran an experiment where human subjects were asked to produce straight lines as fast as possible in different directions. The velocity profile corresponding to each of these lines was then computed, and an analysis-by-synthesis experiment was conducted using the different symbolic models proposed in the scientific literature for describing this type of movement, plus a set of other analytic models that we proposed as potential candidates for describing the phenomenon. Thus, for each line and for each model, we came up with a set of parameters that minimized the error between the original and the reconstructed data, and all the model performances were compared in terms of reconstruction errors. This paper reports on this experiment.

## 2 Modelling of the movement generation system

The modelling of the movement generation system, from the central nervous system down to the hand, has been proposed as a way to globally understand the phenomena related to trajectory formation. But, when developing their models, researchers did not have the same goal, and so these models were of different design. A survey of the previously published models of the movement generation system revealed that the authors mainly had two interests:

*a)* The physical aspects of the system (muscle geometry, mechanical properties, etc.)

*b)* The control processes of the system involved in the trajectory formation

In the first category of models (called *dynamic-oriented models* below) are included those for which the mechanism of trajectory formation is directly related to the geometry of the muscles and to their mechanical properties (Morasso and Mussa-Ivaldi 1982). These models consider the movement generation system to comprise two levels: a cognitive/symbolic (high) level and a joint/muscular (low) level. The high level is assumed to be for coding and planning. The low level contains a geometrical and mechanical transformation mechanism, the high level a decision execution mechanism (van Galen 1980). In this group, three subclasses can be distinguished: models considering the muscles as force generators, as oscillation generators, and as speed generators.

The second category of models (called *kinematic-oriented models* below) are those for which the trajectory formation mechanism is independent of the actual joint and muscle patterns, and are based on the capability of expressing and controlling the trajectory of the hand in space. This hypothesis can be explained by logical reasoning (Lashley 1951; Bernstein 1967) or by well-known facts, e.g., people can write in almost the same way on paper or on a blackboard using the hand or the foot (Katz 1951). These models also rely on the fact that the kinematic patterns of the hand are invariant with respect to variations of starting point, of inclination and of size (Abend et al. 1982; Morasso 1981). To represent the mechanisms of movement generation, kinematic-oriented models consider a three-level system in which an intermediate level for information processing is added to the two previous levels of the dynamic-oriented models. This intermediate level is used to generate spatio-temporal patterns for a given planned movement and to transform spatial sequences into angular/muscular sequences.

In our study, we have analyzed all these models with a fixed point of view, which is their performance in reproducing the velocity profile of simple and rapid aimed-movements. Indeed, many investigators have reported that the velocity profiles of rapid-aimed movements are approximately bell-shaped (Beggs and Howarth 1972; Georgopoulos et al. 1981; Morasso 1981; Soechting and Laquaniti 1981; Abend et al. 1982; Atkenson and Hollerbach 1985). Moreover, the shape of the bell, after appropriate rescaling, is approximately superimposable, that is, the shape is almost preserved for movements that vary in duration, distance or peak velocity (Atkenson and Hollerbach 1985; Bullock and Grossberg 1988). These velocity profiles have also been observed in handwriting, for curvilinear velocity (Morasso and Mussa-Ivaldi 1982; Plamondon et al. 1991) and for angular velocity as well (Plamondon 1989b; Plamondon and Yergeau 1990).

This invariance in the shape of the velocity profiles suggests that velocity might play a key role in movement control, and that the central nervous system might, in one way or another, take this information into account in movement planning. In this context, a general way to look at movement generation is to consider the overall sets of neutral and muscle networks involved in the production of a single rapid movement as a linear system producing a velocity profile from an impulse command $U_0(t - t_0)$ of amplitude $D$ occurring at $t_0$ (Plamondon 1991; Plamondon 1993). In this case, we can write:

$$V(t) = \int_0^t DU_0(t - t_0 - \tau)H(\tau)\,\mathrm{d}\tau \tag{1}$$

$$V(t) = DH(t - t_0) \quad \text{with } t \geqslant t_0 \tag{2}$$

Equation (2) shows that the velocity profile directly reflects the impulse response $H(t - t_0)$ of the global system. Since the generation of different rapid movements involves the activation of the same neuromuscular systems under different experimental conditions, the similarity of the velocity profiles and their invariance for different experimental conditions follows directly (Plamondon 1993). Much indirect evidence also supports this view (Gibson et al. 1985; Houk and Gibson 1987; Plamondon and Parizeau 1988; Houk 1989; Plamondon and Maarse 1989; Plamondon 1992a).

Moreover, we have not limited out study to the set of models already published, but have also extended it to other models that we consider potential candidates for best describing the velocity profiles of rapid movements. For each model, we therefore provide a brief description of its velocity output using the following representation and notation:

$V_\sigma$: curvilinear velocity; $V_\sigma = \sqrt{V_X^2 + V_Y^2}$
$T_0$: time of movement beginning
$T_1$: time of movement end
$T_m$: time of maximum velocity
$P_i$: parameters of the model

The equations of the curvilinear velocity profile produced by each model are listed in the Appendix.

The results of our analysis-by-synthesis experiments are summarized in Table 1. This table, divided into three parts, will be used throughout the paper. In the first column, all the models tested are listed in alphabetical order, grouped into the three families of models (dynamic-oriented models, kinematic-oriented models previously published, new kinematic-oriented models added in this study). The next two columns of this table show the number of parameters for each model as well as some properties of the model. As can be seen, there is great variation between the models in terms of their number of parameters and whether they produce continuous or discontinuous, symmetric or asymmetric velocity profiles.

**Table 1.** Performances of all models studies

| Model | | No of parameters | Properties | MSE (cm²/s²) | Standard deviation | Percentage of lines |
|---|---|---|---|---|---|---|
| EH | Eden (1962)/Hollerbach (1981) | 7 | SC | 5.21 | 6.59 | 95.6 |
| MAR | Maarse (1987) | 12 | AD | 2.01 | 1.39 | 91.4 |
| MCD | MacDonald (1964) | 18 | AD | 12.70 | 12.02 | 97.9 |
| ME | Mermelstein and Eden (1964) | 14 | AD | 0.99 | 2.64 | 97.9 |
| PLA | Plamondon and Lamarche (1986) | 6 | AD | 14.55 | 10.81 | 99.4 |
| DD | Denier van der Gon (1962)/Dooijes (1983) | 12 | AD | 13.49 | 9.91 | 99.4 |
| YAS | Yashuhara (1975) | 9 | AC | 50.35 | 36.21 | 97.6 |
| GOSA | Gaussian asymmetric (Plamondon 1989b) | 6 | AD | 0.49 | 0.51 | 100 |
| GUT | Gutman and Gottlieb original (1991) | 3 | AC | 5.32 | 6.79 | 100 |
| LGN | Lognormal (Plamondon 1991) | 4 | AC | 0.66 | 0.86 | 100 |
| LGNB | Lognormal support-bounded (Plamondon 1992b) | 5 | AC | 0.16 | 0.25 | 100 |
| MJ | Minimum jerk (Flash 1983; Flash and Hogan 1985) | 3 | SC | 1.57 | 1.53 | 100 |
| MMMA | Morasso/Mussa-Ivaldi/Maarse asymmetric (Morasso 1987) | 6 | AD | 1.59 | 1.99 | 98.7 |
| MMMS | Morasso/Mussa-Ivaldi/Maarse symmetric (Morasso 1987) | 3 | SC | 5.30 | 5.79 | 98.4 |
| MOR | Morasso and Mussa-Ivaldi (1982) | 3 | AC | 2.99 | 1.96 | 100 |
| MS | Minimum Snap (Flash 1983; Edelman and Flash 1987) | 3 | SC | 1.33 | 1.49 | 97.8 |
| BET | Beta | 5 | AC | 0.52 | 0.46 | 97.8 |
| GAM | Gamma | 4 | AC | 3.62 | 3.12 | 99.4 |
| GOSS | Gaussian symmetric | 3 | SC | 1.37 | 1.41 | 100 |
| GUTG | Gutman and Gottlieb generalized | 4 | AC | 1.12 | 1.12 | 100 |
| SIGC | Sigmoidal continuous | 4 | AC | 2.56 | 2.29 | 99.1 |
| SIGD | Sigmoidal discontinuous | 8 | AD | 0.81 | 0.58 | 99.1 |
| WBL | Weibull asymmetric | 3 | AC | 97.41 | 61.79 | 100 |

A, Asymmetric; C, continuous; D, discontinuous; S, symmetric

### *2.1 Dynamic-oriented models*

The upper part of Table 1 lists the seven dynamic-oriented models that we have implemented. As may be seen, we have grouped some models together. Although some of these had slight inherent differences, they all led to a similar equation describing the curvilinear velocity profile of the straight lines used in this study, once a simple impulse command had been applied to their specific impulse response.

*The Denier van der Gon and Dooijes models.* The model proposed by Denier van der Gon was the first handwriting model (Denier van der Gon et al. 1962). It considers the fast movement to be caused by two perpendicular groups of muscles which apply forces to the hand to produce the trajectory. The forces generated by the muscles have a rectangular profile and represent the input of a movement generation system described by a second-order equation that takes into account the intrinsic viscosity of the hand. The duration is related to the magnitude of the movement.

Dooijes (1983) tried to improve on the model of Denier van der Gon by proposing two additions: the first was a uniform trend added to the horizontal movement, and the second assumed that the principal axes of direction were oblique rather than orthogonal.

In our study, since we focus on the curvilinear velocity profile, the direction of the principal axis has no influence. Since we also study small movements from a central origin, the uniform trend is not necessary to reproduce the data. In this context, these two models have the same formulation for the asymmetric discontinuous curvilinear velocity profile.

*The MacDonald model.* To improve the performance of the Denier van der Gon/Dooijes model in simulating handwriting, MacDonald (1964) suggested the use of a trapezoidal force pulse. In this case, too, the profile of the curvilinear velocity can be asymmetric and discontinuous.

*The Yasuhara model.* Yasuhara (1975) demonstrated that exponential transitions for the force patterns are even more powerful in the simulation of handwriting. Thus, the force pulses used in this model have an exponential profile and the resulting curvilinear velocity is asymmetric and continuous.

*The Maarse model.* In a model comparison experiment, Maarse (1987) used, among other things, triangular acceleration pulses as input to a cascade of integrators, which is equivalent to assuming a purely ballistic system. The triangular acceleration pulses produce an asymmetric discontinuous velocity profile defined by a second-order polynomial.

*The Eden, Mermelstein and Hollerbach models.* Three authors have proposed a model that considers the muscles as harmonic oscillators. Eden (1962) was the first to suggest such a model, in which the outputs of the movement generation system are sinusoids representing the velocity. In his model, two orthogonal generators of different frequencies are used to simulate handwriting. Mermelstein and Eden (1964) modified this model to incorporate asymmetry in the velocity output by taking into account different amplitudes, frequencies and phase shifts for the rise and fall phases of the profile.

Hollerbach (1981) proposed a synthetic oscillation theory of handwriting. He considered that "handwriting arises from orthogonal oscillations horizontal and vertical in the plane of the writing surface... The oscillations are modulated in certain ways and at specific points to produce the shapes characteristic of the English Palmer script" (p. 140). He studied nonorthogonal axes as well.

The Eden model and the orthogonal axis version of the Hollerbach model used a symmetric continuous curvilinear velocity profile, while the Mermelstein and Eden model used an asymmetric discontinuous velocity profile.

*The Plamondon and Lamarche model.* Another approach was used by Plamondon and Lamarche (1986) to develop a dynamic-oriented model by considering the muscles as speed generators. In fact, they apply the transfer function of the DC motor used in the handwriting simulator of Vredenbregt and Koster (1971) to obtain a speed generator system which produces movement from a rectangular neural pulse and which is independent of the direction (Plamondon 1987, 1989a). The curvilinear velocity profile of such a system is asymmetric and discontinuous.

### 2.2 Kinematic-oriented models

The middle part of Table 1 lists the nine previously published kinematic-oriented models, while the lower part of the table gives seven other potential models.

*The Morasso and Mussa-Ivaldi model.* Morasso and Mussa-Ivaldi (1982) developed a model in which the movement is considered to be a sequence of basic segments of given length, tilt angle and angular change. Each basic stroke is generated with a symmetric continuous bell-shaped velocity profile in its original version. The bell-shaped velocity profile is obtained by a cubic spline function.

*The Flash and Hogan minimum jerk model and the Edelman and Flash minimum snap model.* Dynamic optimization (Nelson 1983; Hogan 1984) has been proposed as a principle of organization for a large class of movements. From this principle, many models have been developed based on the minimizing of one criterion or another. An example is the minimum jerk model (Flash 1983; Flash and Hogan 1985), which considers the trajectory of the movement to be obtained by minimizing the jerk which is the third-time derivative of the displacement. This criterion gives a trajectory defined by a fifth-order polynomial. Another example is the minimum snap model (Flash 1983; Edelman and Flash 1987), which is based on the optimization of the snap (the fourth-time derivative of the displacement) and which gives a trajectory defined by a seventh-order polynomial. The curvilinear velocity profile produced by these two models is symmetric and continuous.

*The Morasso, Mussa-Ivaldi and Maarse models.* In his model comparison experiment, Maarse (1987) described a modified version of the Morasso and Mussa-Ivaldi model (1982) using cosine functions instead of splines for the bell-shaped velocity profile. Two versions of this model are implemented (producing symmetric continuous and asymmetric discontinuous velocity profiles).

*The Plamondon gaussian model.* Plamondon proposed a model based on the intrinsic representation of handwritten curves without reference to any fixed-axis system (Plamondon 1989b). The generation of straight lines is reduced to the production of the curvilinear velocity having an asymmetric discontinuous bell-shaped profile that is represented by a gaussian function (Plamondon 1989b; Leclerc 1989; Leclerc and Plamondon 1990; Plamondon et al. 1990; Plamondon and Clément 1991).

To study the effect of the asymmetry of the velocity profile, we have added a symmetric continuous version of this model (Table 1, lower part) by using one gaussian function instead of the two used in the previous asymmetric version.

*The Gutman and Gottlieb model.* Gutman and Gottlieb (1991) proposed a model that describes the trajectory of a movement by $x(t) = P_1[1 - e^{-t^3/P_2}]$. We have also generalized this model (Table 1, lower part) by using an equation having the power of $t$ as a parameter, which is more general than to fix it at 3, as in the original model. The two versions of this model produce asymmetric continuous velocity profiles.

*The Plamondon lognormal model.* Plamondon proposed a stochastic model for the origin and the invariance of the bell-shaped velocity profiles for rapid-aimed movements (Plamondon 1991). The model describes these movements as originating from the sequential action of a set of velocity generators working in cascade fashion. Applying the central-limit theorem to describe the converging behavior of such a system, it is shown that velocity profiles can be described by lognormal curves (Aitchinson and Brown 1966) which are asymmetric and continuous.

*The Plamondon support-bounded lognormal model.* Plamondon modified his earlier lognormal model in order to propose a more general explanation of the origin of the asymmetric bell-shaped velocity profiles and to describe them with a lognormal function (Plamondon 1992b). This sequential generation model considers the overall sets of neural and muscle networks involved in the production of a single rapid movement as a linear system producing the proper velocity profile from an impulse command. If the global system is made up of a cascade of $n$ linear subsystems with dependent response times, and if $n$ is sufficiently large, the central theorem applies, and predicts that the impulse response of the global system will tend toward a lognormal curve (Aitchinson and Brown 1966). Experimental results suggest that a support-bounded lognormal gives better results; in other words, the time support of the lognormal function is limited, that is, $V_\sigma(t_1) = 0$, where $t_1$ is the end of the movement time (Plamondon 1992b, c).

*New kinematic-oriented models added in this study.* In addition to the symmetric gaussian model and the generalized Gutman and Gottlieb model that we have already mentioned, we have also studied five other models (Table 1, lower part). The *sigmoidal model* (in two versions, continuous and discontinuous) comes from the study of the first-time derivative of a sigmoid function defined by: $f(t) = t^n/(1 + t^n)$. The *beta model* used a beta distribution (which is asymmetric continuous) as a profile for the curvilinear velocity. It should be noted that this model has a discontinuous time derivative in the right-hand part. The *gamma model* uses a gamma distribution (which is asymmetric continuous) as a profile for the curvilinear velocity. The *Weibull model* uses a Weibull distribution (which is asymmetric continuous) as a profile for the curvilinear velocity.

## 3 Data processing

All the original data came from a previously described experiment (Plamondon et al. 1990; Plamondon et al. 1991). These data are composed of 1262 strokes produced by recording the cartesian pentip trajectory of nine subjects sampled during 2-s periods by a digitizer at a spatial resolution of 0.005 in. (0.127 mm) and a sampling frequency of 119.5 Hz. The subset of data used in our study was limited to 1052 strokes by eliminating from the original data those not corresponding to single movements (one dominant velocity pulse).

Each trajectory is described by two space variables $D_X$ and $D_Y$ as a function of a discrete time variable, $t = 0, 1, 2, \ldots, i, \ldots, T$. To minimize the quantization noise and all the jitters produced by the digitizer, a gaussian low-pass filter was applied.

This gaussian filter was synthesized by cascade uniform filters (Wells 1986), and its choice was motivated by the fact that this unique filter class implies no generation of extra extrema in the filtered signal (Badaud et al. 1986). The filter was designed with a cut-off frequency of about 10 Hz, corresponding to the evaluated spectral frequency of rapid handwriting movements (Schomaker and Teulings 1990).

By applying a transform used by Burr (1982), based on the Fourier series interpolator which gives an approximate response that is optimum in the minimum mean-square error sense, coupled with the Campbell smoothing method (Campbell 1973) to minimize the effects of the boundary discontinuities, a continuous approximation $D_{X_F}(t)$, $D_{Y_F}(t)$ was obtained with a continuous time variable $0 \leqslant t \leqslant T$. This approximation could easily be oversampled at a higher rate if desired.

From there, it was easy to evaluate the cartesian velocities $V_{X_F}(t)$, $V_{Y_F}(t)$, and the intrinsic curvilinear velocity was calculated according to

$$V_\sigma = \sqrt{V_{X_F}^2(t) + V_{Y_F}^2(t)} \qquad (3)$$

The signals $D_{X_F}(t)$, $D_{Y_F}(t)$ and $V_\sigma(t)$ were oversampled at a double rate. This operation generally contributes to a better convergence of the iterative reconstruction process.

For each trial, the curvilinear velocity $V_\sigma(t)$ always grows from a null velocity (rest position) and returns to a null velocity. A segmentation was performed to find the temporal boundaries corresponding to the beginning and to the end of the pentip movement related to the production of the straight line. This operation was done to minimize the number of mathematical operations involved in the reconstruction process.

To reconstruct the velocity profile, we needed to extract several parameters from the curvilinear velocity curves. Searching of the parameters was carried out by minimizing a least-squares criterion. The least-squares method is normally dedicated to linear equations, but it is possible to extend this technique to nonlinear equations (Arbenz and Wohlhauser 1980; Press et al. 1989). This is done by expanding the function in the neighborhood of a point that is an approximate solution. Thus, the computed values are not the parameters, but a correction of the approximate solution. After several iterations, it is possible to converge to the parameter solution that minimizes least-squares errors. To do so, the Levenberg–Marquardt method was used. This technique has become a standard for nonlinear least-squares routines (Press et al. 1989). It is a robust method for parameter extraction with minimization of the sum-of-squares errors. It is a compromise between the Gauss–Newton method and the steepest descent method.

After parameter extraction, we can easily reconstruct velocity profiles with the different equations for each model described in the appendix. Figure 1 contains four examples of such reconstructed velocity profiles.

## 4. Results and discussion

The results of our analysis-by-synthesis experiments are summarized in the last three columns of Table 1. For each model, the mean square error (MSE in $cm^2/s^2$), with its standard deviation, and the percentage of lines for which the parameter extraction process has converged are indicated. The results, ranked in ascending order, are also depicted in Fig. 2.

From Fig. 2 or Table 1, we can see that the support-bounded lognormal model gives the best performance in the reconstruction of the 1052 lines, followed by the beta and the asymmetric gaussian models. Increasing the number of parameters is not necessarily the

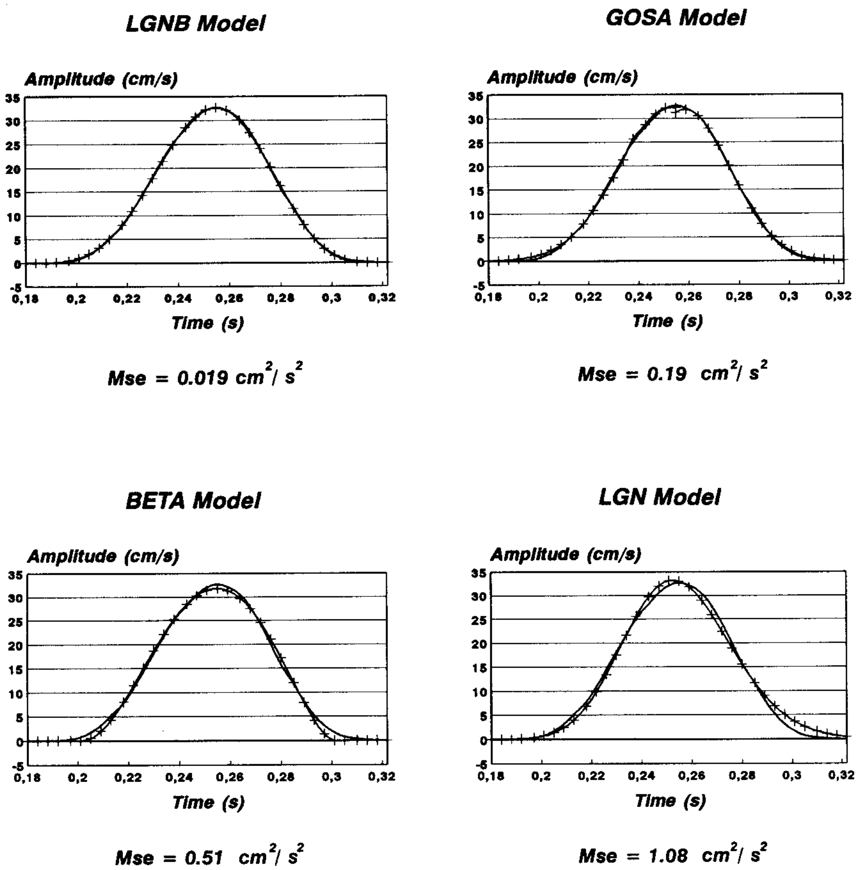


**Fig. 1.** Examples of reconstructed velocity profiles. See Table 1 for full names of models

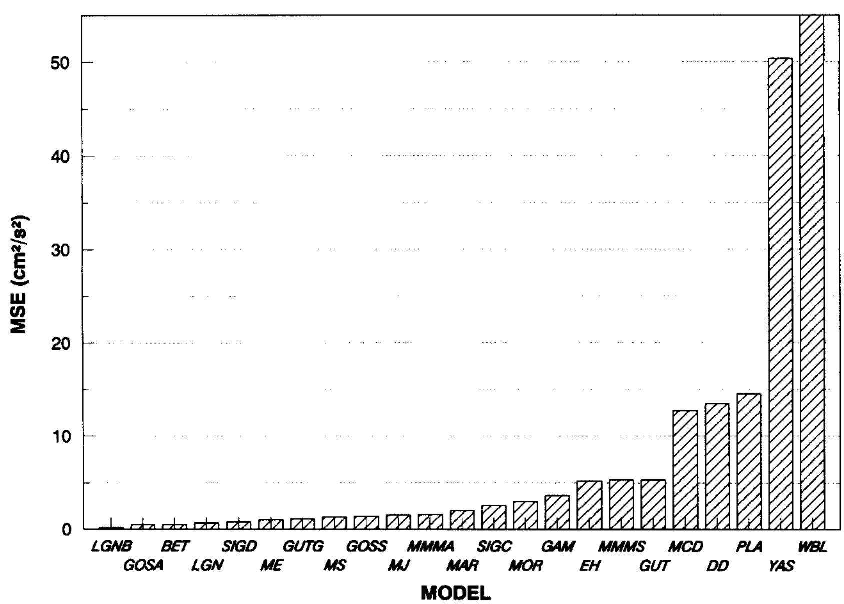


**Fig. 2.** Mean square error of reconstruction of all studied models. See Table 1 for full names of models

way to improve the performances of a model (e.g., the MacDonald model has an MSE = 12.70 $cm^2/s^2$ with 18 parameters, whereas the support-bounded lognormal model gives MSE = 0.16 $cm^2/s^2$ with only 5 parameters, which means that the reconstruction done by using the support-bounded lognormal model is performed with a mean error of only $\pm 0.4$ cm/s over all the velocity profile). Moreover, the complexity of the parameter extraction grows very fast with the number of parameters. Attention should also be paid to the continuity of the velocity profile produced by each model. In fact, real curvilinear velocities are continuous, and a model producing discontinuous profiles is not acceptable even if its performances are high (e.g., the discontinuous version of the sigmoidal model, the beta model and the Mermelstein and Eden model).

From the MSE values given in Table 1, it is not easy to confirm the superiority of one model over another. A statistical analysis is necessary to study the differences between the mean errors calculated over the 1052 lines for the 23 models. For this reason, an unbalanced analysis of variance (ANOVA) was performed on the MSE values of the 23 models, and the test of mean equality was performed by using four different criteria: Wilk's criterion, Pillai's trace, the Hotelling–Lawley trace and Roy's maximum root criterion. According to these studies, two means were said to be different if Prob $> F$ was less than 5%.

Table 2 shows the results of the ANOVA test. As can be seen from this analysis, the global results shown in Table 1 are significant for a majority of models (the boxes in Table 2 show the statistically different successive pairs of models; only seven are not different.

Table 1, clearly shows the great improvement in performance resulting from the use of an asymmetric version of a specific model (the Plamondon gaussian-model GOSA vs GOSS, the Morasso/Mussa-Ivaldi/Maarse model MMMA vs MMMS, the Mermelstein and Eden model ME vs the Eden and Hollerbach model EH). This is in accordance with other findings concerning the universality of the asymmetric bell-shaped velocity profile (Abend et al. 1982; Atkenson and Hollerbach 1985; Morasso 1981; Soechting and Lacquaniti 1981; Nagasaki 1989). Moreover, Beggs and Howarth (1972) have shown that the velocity profile is more symmetric at high speed than at low speed. This asymmetry can even be inverted at very high speed, as reported by Zelaznik et al. (1986). So, an important characteristic of a model should be its facility in providing changes and inversion of the asymmetry. It can be seen from the model equations given in the Appendix that for the support-bounded lognormal model, for example, changing the value of its parameter $P_4$ will directly affect the asymmetry of the velocity profile while a change in the sign of $P_4$ will invert the asymmetry (Plamondon 1993). This feature is difficult to obtain for some of the models (the Gutman and Gottlieb model and the minimum snap model, for example) and is not available for others (the minimum jerk model, the Plamondon gaussian model and the Eden and Hollerbach models, for instance).

Finally, it is observed that the performance of the models is improved in the case of a support-bounded version. For example, in the lognormal model MSE $= 0.66\ cm^2/s^2$ and is the support-bounded version MSE $= 0.16\ cm^2/s^2$.

**Table 2.** Results of ANOVA

| Models compared | $F$ for MSE | Prob $> F$ |
|---|---|---|
| LGNB vs GOSA | $F(1{,}2102) = 354.63$ | 0.001 |
| GOSA vs BET | $F(1{,}2079) = 1.56$ | 0.2113 |
| BET vs LGN | $F(1{,}2079) = 21.12$ | 0.001 |
| LGN vs SIGD | $F(1{,}2092) = 24.14$ | 0.0001 |
| SIGD vs ME | $F(1{,}2070) = 4.82$ | 0.0283 |
| ME vs GUTG | $F(1{,}2080) = 1.92$ | 0.1664 |
| GUTG vs MS | $F(1{,}2079) = 13.74$ | 0.0002 |
| MS vs GOSS | $F(1{,}2079) = 0.32$ | 0.5688 |
| GOSS vs MJ | $F(1{,}2102) = 9.32$ | 0.0023 |
| MJ vs MMMA | $F(1{,}2088) = 0.10$ | 0.7476 |
| MMMA vs MAR | $F(1{,}1998) = 29.46$ | 0.0001 |
| MAR vs SICG | $F(1{,}2003) = 41.88$ | 0.0001 |
| SICG vs MOR | $F(1{,}2093) = 20.46$ | 0.0001 |
| MOR vs GAM | $F(1{,}2096) = 31.19$ | 0.0001 |
| GAM vs EH | $F(1{,}2050) = 49.47$ | 0.0001 |
| EH vs MMMS | $F(1{,}2039) = 0.11$ | 0.7407 |
| MMMS vs GUT | $F(1{,}2085) = 0.00$ | 0.9522 |
| GUT vs MCD | $F(1{,}2080) = 298.64$ | 0.0001 |
| MCD vs DD | $F(1{,}2074) = 2.70$ | 0.1003 |
| DD vs PLA | $F(1{,}2090) = 5.43$ | 0.0199 |
| PLA vs YAS | $F(1{,}2071) = 937.55$ | $< 10^{-4}$ |
| YAS vs WBL | $F(1{,}2077) = 446.12$ | $< 10^{-4}$ |

See Table 1 for full names of models

## 5 Conclusion

In this study, we have used an experimental benchmark to compare different analytical models that have been employed to describe the asymmetric bell-shaped velocity profile universally found in the production of rapid-aimed movements. Using the same experimental approach, all the models have been compared in terms of their performance in reconstructing experimental data from an optimal set of characteristic parameters extracted from these data.

It is clear that the best performances are obtained from a support-bounded lognormal model. The two next best models produce 300% more errors and suffer major discontinuity problems. The fourth best model, an unbounded lognormal, does not encompass discontinuities, but its performances are four times worse than those of the support-bounded version.

In other words, all other models tested go far beyond the support-bounded lognormal, and most of them result in the production of unrealistic velocity profiles, although many of them have been claimed to produce human-like movements. The poor performances of many models seriously question the assumptions made and the conclusions drawn during their development. Their inability to reproduce the data reveals that most of them are inadequate for theoretical purposes and thus should be rejected.

On the other hand, this study strongly suggests that lognormal models should be further investigated in order to throw light on the neuromuscular processes that are hidden behind their analytical description. Apart from being well supported theoretically (Plamondon 1991, 1992b), the lognormal approach supports different asymmetry profiles and is among the models that necessitates a minimal number of parameters for reconstruction. Moreover, it can be used to derive basic laws and trade-offs that occur in human movements (Plamondon 1992b).

Finally, from a practical perspective, the differences in performance among the various models show the importance of running exhaustive comparisons with real data, under a specific reconstruction criterion, before adopting or proposing a new model. Any new model will have to outperform the support-bounded lognormal model to be considered as a potential candidate for analyzing and describing rapid human movements, otherwise it should be rejected.

*Acknowledgements*. This work was supported by grant OGP0915 from NSERC-Canada and grants ER1220 and AS2665 from FCAR-Québec. A. M. Alimi and F. Leclerc received scholarships from ACDI-Canada and Coopération France–Québec respectively. The authors are also grateful to the Ecole Polytechnique, Montréal, for financial support.

## Appendix: equations of curvilinear velocity profile for all models

*The Denier van der Gon and Doojies models*

$$V_\sigma = \begin{cases} \sqrt{[P_1(1-e^{-P_2(t-P_3)})]^2 + [P_4(1-e^{-P_5(t-P_6)})]^2}; & T_0 \leqslant t \leqslant T_m \\ \sqrt{[P_7 e^{-P_8(t-P_9)}]^2 + [P_{10} e^{-P_{11}(t-P_{12})}]^2}; & T_m \leqslant t \leqslant T_1 \\ 0 & \text{elsewhere} \end{cases}$$

*The MacDonald model*

$$V_\sigma = \begin{cases} \sqrt{[P_1(1-e^{-P_2(t-P_3)})]^2 + [P_4(1-e^{-P_5(t-P_6)})]^2}; & T_0 \leqslant t \leqslant T_2 \\ \sqrt{[P_7 e^{-P_8(t-P_{19})} + (P_9 t - P_{19})]^2 + [P_{10} e^{-P_{11}(t-P_{19})} + (P_{12} t - P_{19})]^2}; & T_2 \leqslant t \leqslant T_3 \\ \sqrt{P_{13} e^{-P_{14}(t-P_{15})}]^2 + [P_{16} e^{-P_{17}(t-P_{18})}]^2}; & T_3 \leqslant t \leqslant T_1 \\ 0 & \text{elsewhere} \end{cases}$$

In our simulations, we have taken $T_2 = T_0 + (T_1 - T_0)/6$ and $T_3 = T_1 - (T_1 - T_0)/6$. These values were chosen to obtain a large constant zone in the acceleration pulse as reported in the MacDonald experiments (MacDonald 1964).

*The Yashura model*

$$V_\sigma = \begin{cases} \sqrt{[P_1 e^{-P_2(t-P_9)} + P_3 e^{-P_4(t-P_9)}]^2 + [P_5 e^{-P_6(t-P_9)} + P_7 e^{-P_8(t-P_9)}]^2}; & T_0 \leqslant t \leqslant T_1 \\ 0 & \text{elsewhere} \end{cases}$$

*The Maarse model*

$$V_\sigma = \begin{cases} \sqrt{[P_1(t-P_2)(t-P_3)]^2 + [P_4(t-P_5)(t-P_6)]^2}; & T_0 \leqslant t \leqslant T_m \\ \sqrt{[P_7(t-P_8)(t-P_9)]^2 + [P_{10}(t-P_{11})(t-P_{12})]^2}; & T_m \leqslant t \leqslant T_1 \\ 0 & \text{elsewhere} \end{cases}$$

*The Eden and Hollerbach models*

$$V_\sigma = \begin{cases} \sqrt{\{P_1 \sin[P_2(t-P_3)] + P_4\}^2 + \{P_5 \sin[P_6(t-P_7)]\}^2}; & T_0 \leqslant t \leqslant T_1 \\ 0 & \text{elsewhere} \end{cases}$$

*The Mermelstein and Eden model*

$$V_\sigma = \begin{cases} \sqrt{\{P_1 \sin[P_2(t-P_3)] + P_4\}^2 + \{P_5 \sin[P_6(t-P_7)]\}^2}; & T_0 \leqslant t \leqslant T_m \\ \sqrt{\{P_8 \sin[P_9(t-P_{10})] + P_{11}\}^2 + \{P_{12} \sin[P_{13}(t-P_{14})]\}^2}; & T_m \leqslant t \leqslant T_1 \\ 0 & \text{elsewhere} \end{cases}$$

*The Plamondon and Lamarche model*

$$V_\sigma = \begin{cases} P_1(1-e^{-P_2(t-P_3)}); & T_0 \leqslant t \leqslant T_m \\ P_4 e^{-P_5(t-P_6)}; & T_m \leqslant t \leqslant T_1 \\ 0 & \text{elsewhere} \end{cases}$$

*The Morasso and Mussa-Ivaldi model*

$$V_\sigma = \begin{cases} P_1(t-P_2)(t-P_3); & T_0 \leqslant t \leqslant T_1 \\ 0 & \text{elsewhere} \end{cases}$$

*The Flash and Hogan minimum jerk model*

$$V_\sigma = \begin{cases} P_1(t-P_2)^2(t-P_3)^2; & T_0 \leqslant t \leqslant T_1 \\ 0 & \text{elsewhere} \end{cases}$$

*The Edelman and Flash minimum snap model*

$$V_\sigma = \begin{cases} [P_1(t-P_2)^3(t-P_3)^3; & T_0 \leqslant t \leqslant T_1 \\ 0 & \text{elsewhere} \end{cases}$$

*The symmetric version of the Morasso, Mussa-Ivaldi and Maarse model*

$$V_\sigma = \begin{cases} P_1\{1-\cos[P_2(t-P_3)]\}; & T_0 \leqslant t \leqslant T_1 \\ 0 & \text{elsewhere} \end{cases}$$

*The asymmetric version of the Morasso, Mussa-Ivaldi and Maarse model*

$$V_\sigma = \begin{cases} P_1\{1-\cos[P_2(t-P_3)]\}; & T_0 \leqslant t \leqslant T_m \\ P_4\{1-\cos[P_5(t-P_6)]\}; & T_m \leqslant t \leqslant T_1 \\ 0 & \text{elsewhere} \end{cases}$$

*The asymmetric version of the Plamondon gaussian model*

$$V_\sigma = \begin{cases} P_1\, e^{-((t-P_2)/P_3)^2}; & T_0 \leqslant t \leqslant T_m \\ P_4\, e^{-((t-P_5)/P_6)^2}; & T_m \leqslant t \leqslant T_1 \\ 0 & \text{elsewhere} \end{cases}$$

*The symmetric version of the Plamondon gaussian model*

$$V_\sigma = \begin{cases} P_1(t-P_2)^2\, e^{-((t-P_2)^3/P_3)}; & T_0 \leqslant t \leqslant T_1 \\ 0 & \text{elsewhere} \end{cases}$$

*The original version of the Gutman and Gottlieb model*

$$V_\sigma = \begin{cases} P_1(t-P_2)^2\, e^{-((t-P_2)^3/P_3)}; & T_0 \leqslant t \leqslant T_1 \\ 0 & \text{elsewhere} \end{cases}$$

*The generalized version of the Gutman and Gottlieb model*

$$V_\sigma = \begin{cases} P_1(t-P_2)^{(P_3-1)}\, e^{-((t-P_2)^{P_3}/P_4)}; & T_0 \leqslant t \leqslant T_1 \\ 0 & \text{elsewhere} \end{cases}$$

*The Plamondon lognormal model*

$$V_\sigma = \begin{cases} \dfrac{P_1}{(t-P_2)}\, e^{-P_3[\ln(t-P_2)-P_4]^2}; & T_0 \leqslant t \leqslant T_1 \\ 0 & \text{elsewhere} \end{cases}$$

*The Plamondon support-bounded lognormal model*

$$V_\sigma = \begin{cases} \dfrac{P_1}{(t-P_2)(P_3-t)}\, e^{-P_4[\ln((t-P_2)/(P_3-t))-P_5]^2}; & T_0 \leqslant t \leqslant T_1 \\ 0 & \text{elsewhere} \end{cases}$$

*The continuous version of the sigmoidal model*

$$V_\sigma = \begin{cases} P_1 \dfrac{t-P_2}{[1+P_3(t-P_2)^{P_4}]^2}; & T_0 \leqslant t \leqslant T_1 \\ 0 & \text{elsewhere} \end{cases}$$

*The discontinuous version of the sigmoidal model*

$$V_\sigma = \begin{cases} P_1 \dfrac{t-P_2}{[1+P_3(t-P_2)^{P_4}]^2}; & T_0 \leqslant t \leqslant T_m \\ P_5 \dfrac{t-P_6}{[1+P_7(t-P_6)^{P_8}]^2}; & T_m \leqslant t \leqslant T_1 \\ 0 & \text{elsewhere} \end{cases}$$

*The beta model*

$$V_\sigma = \begin{cases} P_1(t-P_2)^{P_3}(P_4-t)^{P_5}; & T_0 \leqslant t \leqslant T_1 \\ 0 & \text{elsewhere} \end{cases}$$

*The gamma model*

$$V_\sigma = \begin{cases} P_1(t-P_2)^{P_3}\, e^{-P_4(t-P_2)}; & T_0 \leqslant t \leqslant T_1 \\ 0 & \text{elsewhere} \end{cases}$$

*The Weibull model*

$$V_\sigma = \begin{cases} P(t-P_2)^{P_3-1}\, e^{-(t-P_2)^{P_3}}; & T_0 \leqslant t \leqslant T_1 \\ 0 & \text{elsewhere} \end{cases}$$

## References


Abend W, Bizzi E, Morasso P (1982) Human arm trajectory formation. Brain 105:331–348

Arbenz K, Wohlhauser A (1980) Analyse numérique, tome 1. Presses Polytechniques, Lausanne Romande

Aitchinson J, Brown JAC (1966) The lognormal distribution. Cambridge University Press, London

Atkenson CG, Hollerbach JM (1985) Kinematic features of unrestrained vertical arm movements. J Neurosci 5:2318–2330

Badaud J, Witkin AP, Baudin M, Duda RP (1986) Uniqueness of the gaussian kernel for scale-space filtering, IEEE Trans Pattern Anal Machine Intell 8:26–33

Beggs WDA, Howarth CI (1972) The movement of the hand towards a target. Q J Exp Psychol 24:448–453

Bernstein N (1967) The coordination and regulation of movements. Pergamon Press, London

Bullock D, Grossberg S (1988) Neural dynamics of planned arm movements: emergent variants and speed-accuracy properties during trajectory formation. In: Grossberg S (ed) Neural networks and pattern recognition. MIT Press, Cambridge, MA, pp 553–622

Burr DJ (1982) A normalizing transform for cursive script recognition. Proceedings of the 6th International Conference on Pattern Recognition, Munich, pp 1027–1030

Campbell AB (1973) A new sampling theorem for causal (non-band limited) functions. PhD dissertation, University of New Mexico, Albuquerque

Denier van der Gon JJ, Thuring JP, Strackee J (1962) A handwriting simulator. Physics Med Biol 6:407–414

Dooijes EH (1983) Analysis of handwriting movements. Acta Psychol 54:99–114

Edelman S, Flash T (1987) A model of handwriting. Biol Cybern 57:25–36

Eden M (1962) Handwriting and pattern recognition. IRE Trans Inform Theory 8:160–166

Flash T (1983) Organizing principles underlying the formation of arm trajectories. PhD dissertation, Massachusetts Institute of Technology, Cambridge, MA

Flash T, Hogan N (1985) The coordination of arm movements: an experimentally confirmed mathematical model. J Neurosci 5:1688–1703

Georgopoulos AP, Kalaska JF, Massey JT (1981) Spatial trajectories and reaction time of aimed movements: effects of practice, uncertainty, and change in target location. J Neurophysiol 64:725–743

Gibson AR, Houk JC, Kohlerman NJ (1985) Relation between red nucleus discharge and movement parameters in trained macaque monkeys. J Physiol (Lond) 358:551–570

Gutman SR, Gottlieb GL (1991) Exponential model with nonlinear time of reaching movement: trajectory time profile, strategies, variability. Third IBRO World Congress of Neuroscience, Montréal, Canada, August, paper P39.23, p 262

Hogan N (1984) An organizing principle for a class of voluntary movements. J Neurosci 4:2745–2754

Hollerbach JM (1981) An oscillation theory of handwriting. Biol Cybern 39:139–156

Houk JC, Gibson AR (1987) Sensimotor processing through the cerebellum. In: King JJ (ed) New concepts in cerebellar neurobiology. Liss, New York, pp 387–416

Houk JC (1989) Burst of discharge recorded from the red nucleus may provide measures of Gottlieb's excitation pulses. Behav Brain Sci 12:224–225

Katz D (1951) Gestalt psychology. Methuen, London

Lashley KS (1951) The problem of serial order in behaviour. In: Jeffress LA (ed) Cerebral mechanisms in behaviour. Wiley, New York, pp 112–146

Leclerc F (1989) Validation d'un modèle générateur de vitesse à profil gaussien sur des signatures manuscrites. MScA dissertation, école polytechnique, Montréal

Leclerc F, Plamondon R (1990) Validation d'un modèle de la fonction de transfert du bras sur des signatures manuscrites. Proceedings Vision Interface '90, pp 105–111

Maarse F (1987) The study of handwriting movement. PhD dissertation, University of Nijmegen, The Netherlands

MacDonald JS (1964) Experimental studies of handwriting signals. PhD dissertation, Massachusetts Institute of Technology, Cambridge, MA

Mermelstein P, Eden M (1964) Experiments on computer recognition of connected handwritten words. Inform Contr 7:225–270

Morasso P (1981) Spatial control of arm movements. Exp Brain Res 42:223–227

Morasso P, Mussa-Ivaldi FA (1982) Trajectory formation and handwriting: a computational model. Biol Cybern 45:131–142

Nagasaki H (1989) Asymmetric velocity and acceleration profiles of human arm movements. Exp Brain Res 74:319–326

Nelson WL (1983) Physical principles for economies of skilled movements. Biol Cybern 46:135–147

Plamondon R (1987) What does differential geometry tell us about handwriting generation? Proceedings of the 3rd international symposium on handwriting and computer applications, Montréal, pp 11–13

Plamondon R (1989a) A handwriting model based on differential geometry. In: Plamondon R, Suen CY, Simner ML (eds) Computer recognition and human production of handwriting. World Scientific, Singapore, pp 179–192

Plamondon R (1989b) Handwriting control: a functional model. In: Cotterill MJR (ed) Models of brain function. Cambridge University Press, Cambridge, UK, pp 563–574

Plamondon R (1991) On the origin of asymmetric bell-shaped velocity profiles in rapid-aimed movements. In: Stelmach GE, Requin J (eds) Tutorials in motor neuroscience. Kluwer, Dordrecht, pp 283–295

Plamondon R (1992a) A model-based segmentation framework for computer processing of handwriting. Proceedings of the 11th Conference on Pattern Recognition, The Hague, pp 303–312

Plamondon R (1992b) A theory of rapid movements. In: Stelmach GE, Requin J (eds) Tutorials in motor behavior II. Elsevier, Amsterdam, pp 55–69

Plamondon R (1993) Looking through handwriting generation from a velocity control perspective. Acta Psychol 82:89–101

Plamondon R, Clément B (1991) Dependence of peripheral and central parameters describing handwriting generation on movement direction. Hum Mov Sci 10:193–221

Plamondon R, Lamarche F (1986) Modelization of handwriting: a system approach. In: Kao HSR, van Galen GP, Hoosain R (eds) Graphonomics: contemporary research in handwriting. Elsevier, Amsterdam, pp 169–183

Plamondon R, Maarse FJ (1989) An evaluation of motor models of handwriting. IEEE Trans Systems Man Cybern 19:1060–1072

Plamondon R, Parizeau M (1988) Signature verification from position velocity and acceleration signals: a comparative study. Proceedings of the 8th international conference on pattern recognition, Rome, pp 260–265

Plamondon R, Yergeau P (1990) A system for the analysis and synthesis of handwriting. Proceedings international workshop on frontier in handwriting recognition, Montréal, pp 105–111

Plamondon R, Stelmach GE, Teasdale N (1990) Motor program coding representation from a handwriting generator: the production of line responses. Biol Cybern 63:443–451

Plamondon R, Li-de Yu, Stelmach GE, Clément B (1991) On the automatic extraction of biomechanical information from handwriting signals. IEEE Trans Systems Man Cybern 21:90–101

Press WH, Flannery BP, Teukolsky SA, Vetterling WT (1989) Numerical recipes in C. Cambridge University Press, Cambridge, UK

Schomaker RB, Teulings HL (1990) A handwriting recognition system based on the properties and architectures of the human motor system. Proceedings international workshop on frontier in handwriting recognition, Montréal, pp 195–209

Soechting JF, Lacquaniti F (1981) Invariant characteristics of a pointing movement in man. J Neurosci 1:710–720

Van Galen GP (1980) Handwriting and drawing: a two stage model of motor behaviour. In: Stelmach GE, Requin J (eds) Tutorials in motor behaviour. North-holland, Amsterdam, pp 567–578

Vredenbregt J, Koster WG (1971) Analysis and synthesis of handwriting. Philips Tech Rev 32:73–78

Wells W (1986) Efficient synthesis of gaussian filters by cascaded uniform filters. IEEE Trans Pattern Anal Machine Intell 8:234–239

Yasuhara M (1975) Experimental studies on handwriting process. Rep Univ Electro Comm 25:233–254

Zelaznik HN, Schmidt RA, Gielen SCAM (1986) Kinematic properties of rapid-aimed head movements. J Motor Behav 18:353–372